Hindawi
International Journal of Photoenergy
Volume 2018, Article ID 9465262, 6 pages
https://doi.org/10.1155/2018/9465262

Research Article

Design, Electrical, and Optical Modelling of Bulk Heterojunction Polymer Solar Cell

Muhammad Ali,[1] **Ahmed Shuja**,[1] **Ahsan Baig**,[1,2] **Erum Jamil**,[1,2] **and Muhammad Amjad**[3]

[1]*Center for Advanced Electronics and Photovoltaic Engineering (CAEPE), International Islamic University, Islamabad 44000, Pakistan*
[2]*Department of Electrical Engineering, International Islamic University, Islamabad 44000, Pakistan*
[3]*Department of Electronics Engineering, Islamia University of Bahawalpur, Bahawalpur 63100, Pakistan*

Correspondence should be addressed to Muhammad Ali; muhammadali@iiu.edu.pk

Received 31 July 2018; Accepted 11 November 2018; Published 19 December 2018

Academic Editor: Kei Ohkubo

The energy scenario today is focused on the development and usage of solar cells, especially in the paradigm of clean energy. To readily create electron and hole pairs, solar cells utilize either photoactive or photosensitive components. A bulk heterojunction (BHJ) is a nanolayer consisting of donor and acceptor components with a large interpenetrated acceptor and donor contact area. In this context, a mix of P3HT and PCBM offers novelty for its use as an acceptor as well as a donor. In the work presented here, we address the mechanism of modelling and characterization of a BHJ-based polymer solar cell. Here, a new design of BHJ polymer solar cells have been designed, modelled, using Silvaco TCAD in the Organic Solar module, and matched with an already assembled device having similar features. Using this model, we have been able to estimate key parameters for the modelled devices, such as the short-circuit current density, open-circuit voltage, and fill factor with less than 0.25 error index compared to the fabricated counterpart, paving the way for fabless polymer solar cell design and optimization.

1. Introduction

Recently, there is a keen interest in developing electronic devices consisting of organic materials [1]; the examples of which include thin film transistors, memory devices, and LEDs as well as solar cells. The reason for this interest is their greater flexibility as well as easier fabrication, especially over large areas, along with the lower production cost [2, 3]. Of special consideration are polymer photovoltaic solar cells (PSCs) [4], which traditionally contain 3 tiers: (a) polymer zone (for photon absorption), (b) region for the production of electron and hole pairs, and (c) a layer for the charges to be carried through to the contacts.

The BHJ-PSC is a developing technology because it offers improved power conversion efficiency [5, 6]; amongst the BHJ-PSC, the P3HT:PCBM devices have been researched in greater depth [7–9]. It is, therefore, vital to analyse the connection between the organic blend layer and the electrode to estimate the overall performance of the BHJ-PSCs [10]. One problem they face is that of charge buildup, which leads to recombination loss and is dominant with nonohmic contacts [11]. The traditional method of addressing it is by using ohmic contacts. Even so, to develop devices with better performance efficiency, dedicated charge extraction layers (CELs), sandwiched between organic blend layer and electrode, are employed, which facilitate the selective extraction of photogenerated carriers to respective electrodes [12, 13].

We keep in mind that organic polymer components are allowed to be donor- or acceptor-based and also have the flexibility to be doped by p-type or n-type impurities. Therefore, they are the perfect alternatives for semiconductor material [14]. Meanwhile, CELs can also be generalized into two different types: electron extraction layers (EELs) and hole extraction layers (HELs), which have to be chosen carefully for optimal device performance. As an example, for donor-acceptor systems, zinc oxide (ZnO) and titanium oxide (TiO_2) are the favoured EEL materials due to their low work functions, which help the carriage of

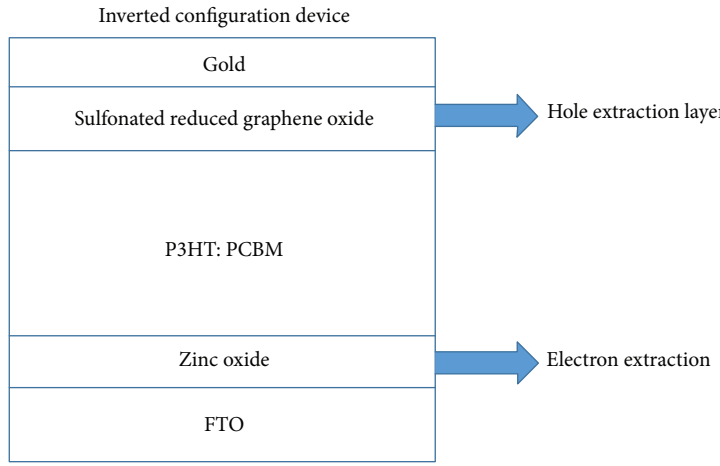

Figure 1: Schematic of the P3HT:PCBM device.

electrons in and out of different electro-optical devices [15]. For HELs, however, the search for an efficient, cost-effective, and easy-to-fabricate HEL is still going on. While one novel material, used widely in organic photovoltaics, for HEL is poly (3,4-ethylenedioxythiophene)-poly(styrenesulfonate) (PEDOT:PSS), its inclination to absorb water and resistance to bar electrons create an issue, while also showing inhomogeneous electro-optical behaviour leading to an ongoing search for new HEL materials [16–18]. In this instance, while the use of graphene-based materials is proving to be a viable option for creating HEL in many solar cell applications [19–21], the use of graphene as a stand-alone material leads to issues due to its zero bandgap. In its stead, the introduction of sulfonated functionalized graphene materials, e.g., graphene oxide and sulfonated graphene oxide [22–24], offers greater adaptability of bandwidth.

Recently, Ali et al. [25] have demonstrated groundbreaking work which demonstrates different P3HT:PSC devices which use different reduced sulfonated graphene oxide (rSGO) as the HEL. Their work shows that with different recipes of rSGO, the electro-optical properties can be customized, by modifying the bandgap. By using the different variants of the rSGO, they were able to demonstrate that the variation of the sulphur and oxygen content allows for the efficient hole extraction and transport.

While the work of [25] provides us the experimental methods of using the sulfonated graphene-based solar cells, there is a need to streamline this process for the purpose of optimization and time-saving capabilities. In this work, therefore, we will demonstrate the development of the fabless model for P3HT:PSC, using Organic Solar, a modelling tool developed by Silvaco TCAD. Further along, we will discuss the starting conditions, as well as the optimization of the parameters. Finally, the results of our modelling will be discussed in comparison with the experimental devices tested in [25].

2. Structural Design

The structure of the BHJ polymer solar cell we consider here comprises five layers, as shown in Figure 1. These are the anode made of fluorine-doped tin oxide, FTO, electron extraction layer using ZnO, photoactive organic layer utilizing P3HT:PCBM, and hole extraction layer making use of sulfonated reduced graphene oxide as well as a gold cathode. The use of FTO as a substrate is justified by its optical transparency along with wide bandgap and low electrical resistivity characteristics of ZnO [26, 27]. Moreover, it also has the property of higher carrier density [28, 29] and various fabrication and implementation recipes, routines, and applications of FTO have been developed over the years [30–37]. In our design, the anode consists of FTO and therefore provides a connection for the flow of anions out of the device. The electron transport layer is a semiconductor layer employed as an electron absorber and charge carrier using TiO_2 and ZnO. Traditionally, a dense n-type compact layer of TiO_2 is deposited on FTO/ITO used as a hole blocking layer, where a mesoporous layer of TiO_2 is used. The efficiency of the polymer solar cell can be improved by blocking the direct recombination that may occur at the interface between perovskite and the FTO. This is usually done by introducing a hole blocking layer between the two materials.

The photons, after having acquired enough energy, travel to the P3HT:PCBM active area where the electron hole pair is then created. For the BHJ, the acceptor part of the junction is the P3HT, while the donor part is the PCBM. Upon the incidence of solar radiations, electron-hole pairs are generated from the P3HT:PCBM blend; whereas the electrons move towards ZnO (i.e., electron extraction layer); the holes move towards reduced graphene oxide (r-SGO) layer (i.e., hole extraction layer). This process is depicted in Figure 1. Further along, they pass through the charge selective layers and are then extracted by the anode and cathode. To understand the optical and electrical properties of such a device, we make use of the simple diode circuit [38], depicted in Figure 2. Here, an important adjustment needs to be made, which is when photons of a particular wavelength and intensity impinge on the diode surface, it responds as a current source dependent on the incoming parameters. Using this model, we can obtain key parameters for the characterization of the solar

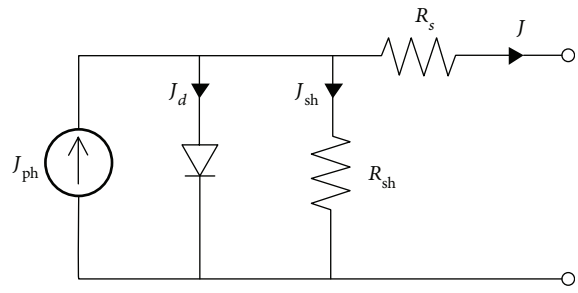

Figure 2: The equivalent circuit for a photovoltaic cell [38].

Table 1: Materials under test as the hole extraction layer [25].

Material	Bandgap (eV)
Reduced sulfonated graphene oxide (rSGO-1)	1.12
Reduced sulfonated graphene oxide (rSGO-2)	1.38
Reduced sulfonated graphene oxide (rSGO-3)	1.44

cells such as short-circuit currents, open-circuit voltage, and fill factor as well as the solar cell efficiency [38].

3. Modelling

The objective of our work is to develop the modelling methodology for the emulation of the physical device. For this purpose, we analysed three devices with varying bandgaps for the HEL and consisting of reduced sulfonated graphene oxides such as rSGO-1, rSGO-2, and rSGO-3. The aim here is to recreate the physical layers of the device as demonstrated in [25] and then use the transport equations to obtain the current density as a function of the solar cell voltage for these devices. The modelling analysis was performed using Organic Solar module along with the Atlas Simulator (both part of the Silvaco TCAD suite), for the materials under test listed in Table 1. The results from the modelling, i.e., the J-V analysis, are then compared with the J-V curves obtained from the characterization of the physically implemented solar cell [25].

The modelling of the P3HT:PSC device requires us to choose a reasonable starting point for the numerical iteration. While the EEL and HEL can be changed in Athena and Silvaco, the cross-sectional area of the solar cell was kept at 1 cm^2, the HEL = 20 nm, EEL = 50 nm, and photoactive la yer = 200 nm thick, by keeping in mind the physical device tested in [25]. Before we model our device, we consider the mesh of the design under consideration. This is an important parameter as it requires grid intersection points (called nodes), which is where the mathematical models are used to obtain vital parameters of the designed device. These nodes are important to optimize because they directly impact the time required for the model to run as well as its precision. The general rule of thumb is that the mathematical operation needed for achieving a solution can be described as

$$\text{Number of mathematical operations} = (\text{Np})^{\alpha}, \quad (1)$$

where Np is defined as the number of nodes, and α is the iteration parameter (usually of the order of 1.5–2.0) [39]. It is also important to keep in mind that we ensure adequate mesh density in areas with high field as well as to avoid discontinuities in the mesh density. The mobility model that we utilized to estimate the device characteristics is the Poole-Frenkel model [40, 41] in combination with the Langevin recombination model [42] for our devices. This is because these are the models traditionally used for BHJ devices. As part of the verification process, the method was first tested for a solar cell suggested by Koster et al. [43, 44], with our modelling technique following the procedures set in place by Organic Solar. After verifying that the response of the modelling is in line with the experimental techniques, we proceeded to the development of the P3HT:PSC device. The main challenge during the modelling was the repetitive iteration required to obtain a numerical solution for the figures of merit. This required the knowledge of work functions of the materials used to fabricate the device, which for some materials, such as ZnO and TiO_2, was a constant. Thus, we ran different iterations to minimize the error function of the HOMO and LOMO energy levels, binding energies, generation rate, bandgaps, affinity, permittivity, and electron and hole mobility as well as the work function, amongst others. By doing this extensively, we obtained the estimated values for the parameters that will be presented shortly.

Table 2: The parameters of the experimental device [25].

HEL materials	V_{oc} (V)	J_{sc} (mA/cm^2)	FF	η (%)
rSGO-1	0.58	5.77	0.46	1.54
rSGO-2	0.60	7.54	0.62	2.80
rSGO-3	0.59	8.29	0.57	2.79

4. Results and Discussion

The figures of merit that we used to analyse the performance of the photovoltaic organic solar cell are the current density, the cell voltage, and the fill factor as well as the solar cell efficiency. These have been listed in Table 2 for the physical devices under test.

The parameters found for the modelled devices are presented in Table 3. Here, we present not only the open-circuit voltage and the short-circuit current density but also other key parameters such as the maximum power output for such devices.

We also present here the relative error in calculation for the modelled and the experimental devices. This is done for all the devices under test and is presented in Table 4. As can be seen, the error in the estimation, compared to the experimental results, is less than 0.15 for almost all of the parameters tested, apart from a few exceptions, showing that as a first approximation, our modelling technique works very well and can be used to design organic solar cells with both electron and hole extraction layers. Here we note that the error index for the solar efficiency, between the modelled and fabricated devices, is greater than all other parameters because it encompasses all the deviations in J-V curves used to calculate the maximum power delivered.

Table 3: The parameters of modelled devices via Silvaco TCAD.

HEL materials	J_{max} (mA/cm^2)	V_{max} (V)	P_{max} (mW)	V_{oc} (V)	J_{sc} (mA/cm^2)	Pout (mW)	η (%)	FF
rSGO-1	3.80	0.26	0.93	0.44	6.50	2.92	0.75	0.39
rSGO-2	5.43	0.40	2.17	0.64	8.30	5.32	1.74	0.71
rSGO-3	5.19	0.42	2.18	0.62	8.32	5.17	1.75	0.61

Table 4: Relative error between the experimental and modelled results.

HEL materials	Absolute error index			
	V_{oc} (V)	J_{sc} (mA/cm^2)	η (%)	FF
rSGO-1	0.240	0.120	0.51	0.152
rSGO-2	0.068	0.101	0.38	0.1451
rSGO-3	0.052	0.003	0.37	0.070

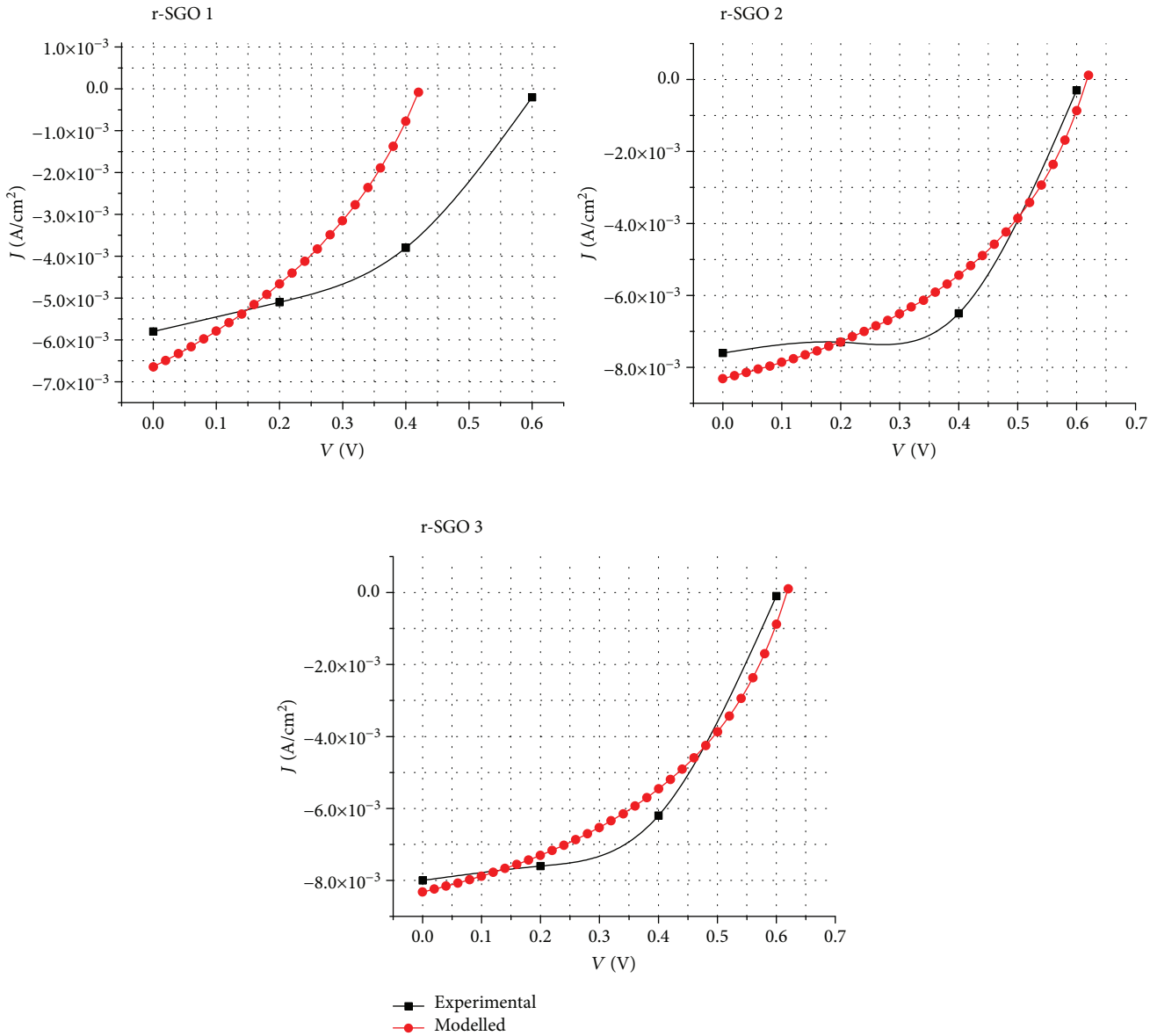

Figure 3: The experimental and modelled current density as a function of solar voltage for the devices under test.

The experimental and modelled current densities as a function of the cell voltage have been depicted in Figure 3. We note here that, although Silvaco allows for variation of the HEL and EEL work functions, we kept them constants for simplicity. The fabrication of the device structure (Figure 1) includes physical defects, environmental factors, and grain boundaries associated with the material in its pristine form as well as restructured during the subsequent processing. This is likely to alter some of the conditions which are usually taken fixed while modelling the structures/device within the theoretical framework/governing design laws.

5. Conclusions

Three different BHJ-based polymer solar cells have been designed and tested, against similar fabricated device, for the output characteristics, and the data extracted, to subsequently analyse them. We also characterized the electro-optical properties of the device which includes the current density and cell voltages, power analysis, and fill factor as well as the photo efficiency. Moreover, the relative error indexes for the prominent figures of merit have also been presented which show that the model estimates almost all of the figures of merit in the experimental data with less than 20% error in calculations. The advantage of doing this is that the postdesign analysis and optimization become much easier and convenient. Moreover, we now have the mechanism in place to test variations of presented device much more quickly and in a cost-effective way than earlier.

Data Availability

The data used to support the findings of this study are included within the article.

Conflicts of Interest

The authors declare that no competing interests exist in the presentation of this work.

Acknowledgments

Mr. Asghar Ali [25] is acknowledged for fabricating the polymer solar cell with similar structural design as of this work for comparison.

References

[1] Y. Shirota, "Organic materials for electronic and optoelectronic devices," *Journal of Materials Chemistry*, vol. 10, no. 1, pp. 1–25, 2000.

[2] B. O'Regan and M. Grätzel, "A low-cost, high-efficiency solar cell based on dye-sensitized colloidal TiO_2 films," *Nature*, vol. 353, no. 6346, pp. 737–740, 1991.

[3] M. M. Lee, J. Teuscher, T. Miyasaka, T. N. Murakami, and H. J. Snaith, "Efficient hybrid solar cells based on meso-superstructured organometal halide perovskites," *Science*, vol. 338, no. 6107, pp. 643–647, 2012.

[4] C. Kamble, N. Chide, S. Mhatre, and S. Sukhdeve, "Thin film organic solar cell as an emerging PV technique," in *2013 International Conference on Green Computing, Communication and Conservation of Energy (ICGCE)*, pp. 649–653, Chennai, India, 2013.

[5] J. You, L. Dou, K. Yoshimura et al., "A polymer tandem solar cell with 10.6% power conversion efficiency," *Nature Communications*, vol. 4, no. 1, p. 1446, 2013.

[6] Y. Liu, J. Zhao, Z. Li et al., "Aggregation and morphology control enables multiple cases of high-efficiency polymer solar cells," *Nature Communications*, vol. 5, no. 1, p. 5293, 2014.

[7] M. T. Dang, L. Hirsch, and G. Wantz, "P3HT:PCBM, best seller in polymer photovoltaic research," *Advanced Materials*, vol. 23, no. 31, pp. 3597–3602, 2011.

[8] D. Chen, A. Nakahara, D. Wei, D. Nordlund, and T. P. Russell, "P3HT/PCBM bulk heterojunction organic photovoltaics: correlating efficiency and morphology," *Nano Letters*, vol. 11, no. 2, pp. 561–567, 2011.

[9] J. A. Hauch, P. Schilinsky, S. A. Choulis, R. Childers, M. Biele, and C. J. Brabec, "Flexible organic P3HT:PCBM bulk-heterojunction modules with more than 1 year outdoor lifetime," *Solar Energy Materials and Solar Cells*, vol. 92, no. 7, pp. 727–731, 2008.

[10] I. Litzov and C. Brabec, "Development of efficient and stable inverted bulk heterojunction (BHJ) solar cells using different metal oxide interfaces," *Materials*, vol. 6, no. 12, pp. 5796–5820, 2013.

[11] L. M. Chen, Z. Xu, Z. Hong, and Y. Yang, "Interface investigation and engineering – achieving high performance polymer photovoltaic devices," *Journal of Materials Chemistry*, vol. 20, no. 13, pp. 2575–2598, 2010.

[12] T.-H. Lai, S.-W. Tsang, J. R. Manders, S. Chen, and F. So, "Properties of interlayer for organic photovoltaics," *Materials Today*, vol. 16, no. 11, pp. 424–432, 2013.

[13] S. Lattante, "Electron and hole transport layers: their use in inverted bulk heterojunction polymer solar cells," *Electronics*, vol. 3, no. 1, pp. 132–164, 2014.

[14] M. Reyes-Reyes, D. L. Carroll, W. Blau, and R. López-Sandoval, "Materials and devices for organic electronics," *Journal of Nanotechnology*, vol. 2011, Article ID 589241, 2 pages, 2011.

[15] Y. Zhou, C. Fuentes-Hernandez, J. Shim et al., "A universal method to produce low-work function electrodes for organic electronics," *Science*, vol. 336, no. 6079, pp. 327–332, 2012.

[16] M. Kemerink, S. Timpanaro, M. M. de Kok, E. A. Meulenkamp, and F. J. Touwslager, "Three-dimensional inhomogeneities in PEDOT:PSS films," *The Journal of Physical Chemistry B*, vol. 108, no. 49, pp. 18820–18825, 2004.

[17] Y.-H. Kim, S.-H. Lee, J. Noh, and S.-H. Han, "Performance and stability of electroluminescent device with self-assembled layers of poly(3,4-ethylenedioxythiophene)–poly(styrenesulfonate) and polyelectrolytes," *Thin Solid Films*, vol. 510, no. 1-2, pp. 305–310, 2006.

[18] Z. Zhu, Y. Bai, T. Zhang et al., "High-performance hole-extraction layer of sol–gel-processed NiO nanocrystals for inverted planar perovskite solar cells," *Angewandte Chemie*, vol. 126, no. 46, pp. 12779–12783, 2014.

[19] J. M. Kim, S. W. Seo, D. H. Shin et al., "Ag-nanowires-doped graphene/Si Schottky-junction solar cells encapsulated with another graphene layer," *Current Applied Physics*, vol. 17, no. 8, pp. 1136–1141, 2017.

[20] N. Kim, G. Xin, S. M. Cho, C. Pang, and H. Chae, "Microwave-reduced graphene oxide for efficient and stable hole extraction layers of polymer solar cells," *Current Applied Physics*, vol. 15, no. 9, pp. 953–957, 2015.

[21] G. Jang, W. Yim, Y. H. Ahn, S. Lee, and J.-Y. Park, "Control of device characteristics by passivation of graphene field effect transistors with polymers," *Current Applied Physics*, vol. 16, no. 11, pp. 1506–1510, 2016.

[22] D. He, Z. Kou, Y. Xiong et al., "Simultaneous sulfonation and reduction of graphene oxide as highly efficient supports for metal nanocatalysts," *Carbon*, vol. 66, pp. 312–319, 2014.

[23] J. Liu, Y. Xue, and L. Dai, "Sulfated graphene oxide as a hole-extraction layer in high-performance polymer solar cells," *The Journal of Physical Chemistry Letters*, vol. 3, no. 14, pp. 1928–1933, 2012.

[24] J. Liu, Y. Xue, Y. Gao, D. Yu, M. Durstock, and L. Dai, "Hole and electron extraction layers based on graphene oxide derivatives for high-performance bulk heterojunction solar cells," *Advanced Materials*, vol. 24, no. 17, pp. 2228–2233, 2012.

[25] A. Ali, Z. S. Khan, M. Jamil, Y. Khan, N. Ahmad, and S. Ahmed, "Simultaneous reduction and sulfonation of graphene oxide for efficient hole selectivity in polymer solar cells," *Current Applied Physics*, vol. 18, no. 5, pp. 599–610, 2018.

[26] S. Tongay, K. Berke, M. Lemaitre et al., "Stable hole doping of graphene for low electrical resistance and high optical transparency," *Nanotechnology*, vol. 22, no. 42, article 425701, 2011.

[27] X. Wang, L. Zhi, and K. Müllen, "Transparent, conductive graphene electrodes for dye-sensitized solar cells," *Nano Letters*, vol. 8, no. 1, pp. 323–327, 2008.

[28] K. S. Ramaiah and V. S. Raja, "Structural and electrical properties of fluorine doped tin oxide films prepared by spray-pyrolysis technique," *Applied Surface Science*, vol. 253, no. 3, pp. 1451–1458, 2006.

[29] T. Tesfamichael, G. Will, M. Colella, and J. Bell, "Optical and electrical properties of nitrogen ion implanted fluorine doped tin oxide films," *Nuclear Instruments and Methods in Physics Research Section B: Beam Interactions with Materials and Atoms*, vol. 201, no. 4, pp. 581–588, 2003.

[30] E. Elangovan and K. Ramamurthi, "Studies on micro-structural and electrical properties of spray-deposited fluorine-doped tin oxide thin films from low-cost precursor," *Thin Solid Films*, vol. 476, no. 2, pp. 231–236, 2005.

[31] P. F. Gerhardinger and R. J. Mccurdy, "Float line deposited transparent conductors-implications for the PV industry," *MRS Proceedings*, vol. 426, 1996.

[32] P. M. Gorley, V. V. Khomyak, S. V. Bilichuk, I. G. Orletsky, P. P. Horley, and V. O. Grechko, "SnO_2 films: formation, electrical and optical properties," *Materials Science and Engineering: B*, vol. 118, no. 1–3, pp. 160–163, 2005.

[33] C.-Y. Kim and D.-H. Riu, "Texture control of fluorine-doped tin oxide thin film," *Thin Solid Films*, vol. 519, no. 10, pp. 3081–3085, 2011.

[34] H. Kim, R. C. Y. Auyeung, and A. Piqué, "Transparent conducting F-doped SnO_2 thin films grown by pulsed laser deposition," *Thin Solid Films*, vol. 516, no. 15, pp. 5052–5056, 2008.

[35] T. Maruyama and H. Akagi, "Fluorine-doped tin dioxide thin films prepared by radio-frequency magnetron sputtering," *Journal of the Electrochemical Society*, vol. 143, no. 1, pp. 283–287, 1996.

[36] R. Mientus and K. Ellmer, "Structural, electrical and optical properties of SnO_{2-x}:F-layers deposited by DC-reactive magnetron-sputtering from a metallic target in $Ar–O_2/CF_4$ mixtures," *Surface and Coatings Technology*, vol. 98, no. 1–3, pp. 1267–1271, 1998.

[37] N. Sankara Subramanian, B. Santhi, S. Sundareswaran, and K. S. Venkatakrishnan, "Studies on spray deposited SnO_2, Pd:SnO_2 and F:SnO_2 thin films for gas sensor applications," *Synthesis and Reactivity in Inorganic, Metal-Organic, and Nano-Metal Chemistry*, vol. 36, no. 1, pp. 131–135, 2006.

[38] C. M. Proctor and T.-Q. Nguyen, "Effect of leakage current and shunt resistance on the light intensity dependence of organic solar cells," *Applied Physics Letters*, vol. 106, no. 8, article 083301, 2015.

[39] "ATLAS," http://www.eng.buffalo.edu/~wie/silvaco/atlas_user_manual.pdf.

[40] F. Torricelli and L. Colalongo, "Unified mobility model for disordered organic semiconductors," *IEEE Electron Device Letters*, vol. 30, no. 10, pp. 1048–1050, 2009.

[41] C.-Y. Nam, D. Su, and C. T. Black, "High-performance air-processed polymer–fullerene bulk heterojunction solar cells," *Advanced Functional Materials*, vol. 19, no. 22, pp. 3552–3559, 2009.

[42] I. Hwang, C. R. McNeill, and N. C. Greenham, "Drift-diffusion modeling of photocurrent transients in bulk heterojunction solar cells," *Journal of Applied Physics*, vol. 106, no. 9, article 094506, 2009.

[43] L. J. A. Koster, E. C. P. Smits, V. D. Mihailetchi, and P. W. M. Blom, "Device model for the operation of polymer/fullerene bulk heterojunction solar cells," *Physical Review B*, vol. 72, no. 8, 2005.

[44] https://www.silvaco.com/examples/tcad/section44/example7/index.html.